Earth's Future

RESEARCH ARTICLE
10.1029/2021EF002099

Ocean Sound Propagation in a Changing Climate: Global Sound Speed Changes and Identification of Acoustic Hotspots

Alice Affatati[1,2], Chiara Scaini[1], and Stefano Salon[1]

[1]National Institute of Oceanography and Applied Geophysics–OGS, Trieste, Italy, [2]Department of Ocean and Naval Architectural Engineering, Faculty of Engineering and Applied Science, Memorial University of Newfoundland and Labrador, St. John's, CA, USA

Key Points:

- New data set of global sound speed at the end of XXI century with associated uncertainty: global sound speed generally increases
- Climate-induced sound speed variations are substantial in selected "acoustic hotspots"
- Underwater sound transmission loss is expected to decrease in acoustic hotspots potentially changing anthropogenic and natural soundscapes

Supporting Information:

Supporting Information may be found in the online version of this article.

Correspondence to:

A. Affatati and C. Scaini,
aaffatati@mun.ca;
cscaini@inogs.it

Citation:

Affatati, A., Scaini, C., & Salon, S. (2022). Ocean sound propagation in a changing climate: Global sound speed changes and identification of acoustic hotspots. *Earth's Future*, *10*, e2021EF002099. https://doi.org/10.1029/2021EF002099

Received 26 MAR 2021
Accepted 24 JAN 2022

Abstract Climate change is a relevant threat on a global scale, leading to impacts on ecosystems and ocean biodiversity. A considerable fraction of marine life depends on sound. Marine mammals, in particular, exploit sound in all aspects of their life, including feeding and mating. This work explores the impact of climate change in sound propagation by computing the three-dimensional global field of underwater sound speed. The computation was performed based on present conditions (2006–2016) and a "business-as-usual" future climate scenario (Representative Concentration Pathway 8.5), identifying two "acoustic hotspots" where larger sound speed variations are expected. Our results indicate that the identified acoustic hotspots will present substantial climate-change-induced sound speed variations toward the end of the century, potentially affecting the vital activities of species in the areas. Evidence is provided of the impact of such variation on underwater sound transmission. As an example of a species impacted by underwater transmission, we considered one marine mammal endangered species, the North Atlantic right whale (*Eubalaena glacialis*), in the northwestern Atlantic Ocean. To the best of our knowledge, this is the first global-scale data set of climate-induced sound speed changes expected under a future scenario. This study provides a starting point for policies oriented research to promote the conservation of marine ecosystems and, in particular, endangered marine mammals.

Plain Language Summary Marine fauna, especially cetaceans, depend on sound for all biological functions. Climate change is probably the greatest anthropogenic challenge that humankind faces and it is damaging biodiversity and ecosystems on a global scale. In this work, we coupled these two issues by analyzing future climate change consequences on underwater sound propagation. We based our computations on a high-emissions scenario, which represents a likely outcome if society does not act on reducing greenhouse gas emissions. We calculated global changes in sound speed and identified the areas that will be most affected at the end of the century. We showed the expected changes on sound propagation using as example one endangered cetacean species whose typical calls will undergo changes in future. We conclude that these future sound speed variations will affect marine mammals' communication and other vital activities that rely on sound propagation. To the best of our knowledge, this is the first global-scale assessment of sound speed and its expected future changes. It provides a starting point for policies that promote the conservation of marine ecosystems and, in particular, endangered marine mammals. In addition, it paves the way to investigate the possible combination of such changes with other anthropogenic pressures (e.g., vessel traffic) which might endanger multiple species in the future.

1. Introduction

Climate change is one of the most challenging threats that humankind faces (Reser & Swim, 2011). The global energy imbalance, dominated by ocean warming, was estimated for 2005–2010 by the Intergovernmental Panel on Climate Change Fifth Assessment Report to be 0.6 (±0.4) W/m^2 applied over the entire surface area of the Earth (Johnson & Lyman, 2020). According to a recent Ocean State Report of the EU Copernicus Marine Service (von Schuckmann et al., 2018), in the period 1993–2018, the trend of the global ocean heat content in the 0–700 m layer was estimated to be +0.9 (±0.1) W/m^2, while the global sea surface temperature has increased by 0.014 (±0.001)°C per year. This phenomenon impairs marine ecosystems and organisms, lowering their reproductive rate, impacting their behavior, and triggering shifts in keystone species distribution and ecological interactions (Tittensor et al., 2010; Trisos et al., 2020). Despite all the efforts devoted by the scientific community to assess the expected impacts of climate change on marine ecosystems (Doney et al., 2012; Hoegh-Guldberg & Bruno, 2010), its effect on underwater sound propagation is not widely researched. There are only a few global-scale studies on marine mammals' vulnerability to

global warming (e.g., Albouy et al., 2020), and none of them focused on underwater sound propagation changes. In particular, to the best of our knowledge, there are no quantitative studies on the expected magnitude and distribution of climate-change-induced sound speed variations. Thus, climate-induced sound speed changes, exploiting important acoustic features such as the Sound Fixing and Ranging channel (SOFAR) (Munk et al., 1995) might modify how sound is transmitted underwater. In addition, the impact of such variations on marine mammals' vital activities has not been assessed yet. We believe that this link needs to be explored because a considerable part of life in the ocean depends on sound (Hildebrand, 2009). In fact, cetaceans have become acoustically oriented and have developed highly specialized auditory systems, and these animals need a suitable acoustic environment to thrive (Wartzok et al., 2003). Aquatic mammals are very vocal, and they use sound in a variety of contexts, including competitive manners to show territorial hegemony, to look for food, and to find a partner, but also to warn other individuals about the presence of a predator (Au & Hastings, 2008).

Nowadays, there is an urgent need for conservation efforts to reverse marine life decline, re-establish the ocean ecosystem, and guarantee human well-being (Duarte et al., 2020). In order to establish conservation and sustainable management policies, the scientific community is committed to generating evidence of the magnitude and extent of expected impacts. Without a concerted mitigation action, these impacts could become irreversible, also leading to socioeconomic issues (GEF LME:LEARN, 2017). Therefore, environmental data sets for ocean acoustic variables are urgently needed in order to quantify the expected changes, consider mitigation policies, and support further research.

Based on these premises and driven by these reasons, we perform a global assessment of the climate-change-induced variation of sound speed expected under a "business as usual" high-emission climate scenario known as the Representative Concentration Pathways 8.5 (RCP8.5; van Vuuren et al., 2011). We identify areas where sound speed variations are more prominent (referred to as "acoustic hotspots") and where marine ecosystems might undergo substantial changes. Then, we focus on one selected area and species and compute underwater sound transmission loss for a specific case study, providing evidence of the expected changes in sound transmission and insights on future marine mammals' communication. Finally, we discuss the oceanographic implications of climate-change-induced sound speed variations and the challenges for the ocean's sustainable management and marine ecosystem conservation.

2. Materials and Methods

2.1. Climatic Data

In order to compute the sound speed field, we retrieved three-dimensional (3-D) global ocean data of salinity and temperature for a present and a future decade, from two different data sources (Table 1):

Table 1
Details on Data Sets Used for the Sound Speed Computation

Data set	Provider	Horizontal resolution	Vertical levels (m)	Decade retrieved, temporal resolution
Global ocean physics reanalysis GLORYS2V4 (REAN)	CMEMS	0.25 × 0.25°	75: 0.50, 1.55, 2.66, 3.85, 5.14, 6.54, 8.09, 9.82, 11.77, 13.99, 16.52, 19.42, 22.75, 26.55, 30.87, 35.74, 41.18, 47.21, 53.85, 61.11, 69.02, 77.61, 86.92, 97.04, 108.0, 120.00, 133.07, 147.40, 163.16, 180.54, 199.79, 221.14, 244.89, 271.35, 300.88, 333.86, 370.68, 411.79, 457.62, 508.63, 565.29, 628.02, 697.25, 773.36, 856.67, 947.44, 1045.85, 1151.99, 1265.86, 1387.37, 1516.36, 1652.56, 1795.67, 1945.29, 2101.02, 2262.42, 2429.02, 2600.38, 2776.03, 2955.57, 3138.56, 3324.64, 3513.44, 3704.65, 3897.98, 4093.15, 4289.95, 4488.15, 4687.58, 4888.07, 5089.47, 5291.68, 5494.57, 5698.06, 5902.05	2005–2015, monthly means
CESM large ensemble date sets, member #1 (LENS)	NCAR/UCAR	1 × 1°	60: 5, 15, 25, 35, 45, 55, 65, 75, 85, 95, 105, 115, 125, 135, 145, 155, 165, 176, 186, 197, 210, 222, 236, 251, 267, 285, 305, 326, 351, 378, 408, 443, 482, 527, 579, 638, 707, 787, 879, 985, 1106, 1244, 400, 573, 1764, 1968, 2186, 2413, 2649, 2889, 3133, 3379, 3627, 3876, 4125, 4375, 4625, 4875, 5125, 5375	2006–2016/2090–2100, monthly means

1. The Global Ocean Physics Reanalysis data set (GLObal ReanalisYS V4, GLORYS2V4; Global Monitoring and Forecasting Center, 2018; von Schuckmann et al., 2018; so on referred as "REAN"), produced within the European Copernicus Marine Environment Monitoring Service (CMEMS) with an eddy-permitting model system assimilating satellite (Sea Surface Temperature and Sea Level Anomaly) and in situ (Temperature and Salinity profiles, Sea Ice concentration) data. Ocean reanalysis data sets integrate observations into models and represent the optimal reconstruction of the recent past periods.
2. The climate scenario is the first member of a 40-member ensemble performed using the Community Earth System Model (CESM) version 1 within the CESM Large Ensemble project (LENS; Kay et al., 2015), so on referred to as "LENS." We selected the RCP8.5 climate change scenario, characterized by a rising radiative forcing leading to 8.5 W/m^2 in 2100 (van Vuuren et al., 2011).

The two data sets are available online (references are provided in the Supporting Information S1) together with the corresponding technical documentation which describes the data set features, here summarized in Table 1. Data from the LENS data set were retrieved for the present decade (i.e., the earliest available decade, 2006–2016) and a future decade (2090–2100), respectively referred to as "LENS-pres" and "LENS-futr." We then retrieved the closer available decade from the REAN data set (2005–2015). The gridded data, in netCDF format, were downloaded at the native spatial-temporal resolution (see Table 1). Then, salinity and temperature monthly averages over each selected period were calculated for each cell of the domain, obtaining a climatological year composed of 12 monthly means, for both present and future decades, thus resulting in a three-dimensional data set over the entire global area. All operations on the netCDF data were performed using the NCO (Zender et al., 2012) and CDO (Schulzweida, 2019) packages.

Uncertainty estimates for salinity and temperature were also accounted for at each vertical level z listed in Table 1 ($\Delta S(z)$ and $\Delta T(z)$, respectively). Table 2 summarizes the uncertainty associated with salinity and temperature according to the technical documentation of the two considered data sets (Table 1). In particular, the REAN technical documentation provided the Root Mean Square Difference (RMSD) values for temperature and salinity for specific depth layers. Similarly, for the LENS data set, the technical reference provided values of temperature and salinity average RMSD for the first 8 members of the ensemble, at specific depths. The only minor data manipulation was (a) the interpolation of the uncertainty of temperature and salinity on all the depth levels of the corresponding data sets (75 depth levels for REAN and 60 depth levels for LENS), and (b) the computation of the uncertainty values of the sound speed at each vertical level, following the formula for ΔSS (T, S, z) in Section 2.2. In order to account for the uncertainty variation at intermediate depth levels, a linear interpolation was performed between the available values. ΔT (z) ranges between 0.04° and 1.38°C, while ΔS (z) ranges from 0.01 to 0.83 psu, both generally increasing from REAN to LENS.

Based on such information, 3-D temperature and salinity uncertainty values at each vertical level were added to the original data sets.

Table 2
Temperature (ΔT) and Salinity (ΔS) RMSD Uncertainty Error Values for the Two Considered Data Sets at the Available Vertical Depths

REAN		Depth (m)	0–100			100–300		300–800		800–2000			2000–5000		
	RMSD for each vertical layer	ΔT (°C)	0.68			0.61		0.36		0.12			0.12		
		ΔS (psu)	0.165			0.092		0.049		0.02			0.02		
LENS		Depth (m)	0	50	100	200	300	500	1000	1500	2000	2500	3000	3500	4000
	RMSD at specific depths	ΔT (°C)	0.94	1.07	1.30	1.38	1.22	1.03	0.96	0.62	0.58	0.63	0.66	0.66	0.65
		ΔS (psu)	0.83	0.74	0.60	0.50	0.46	0.38	0.29	0.22	0.21	0.19	0.15	0.12	0.11

2.2. Sound Speed Calculation

A monthly average sound speed (SS) was computed for both present and future decades based on the salinity and temperature data extracted from the data sets presented in Table 1. The calculation was performed for each cell of the data sets' 3-D grid using the MacKenzie formula (Mackenzie, 1981), which has an accuracy of about 0.1 m/s (Dushaw et al., 1993):

$$\mathrm{SS}(T,S,z) = a + \mathrm{bT} + \mathrm{cT}^2 + \mathrm{dT}^3 + e(S-35) + \mathrm{fz} + \mathrm{gz}^2 + \mathrm{hT}(S-35) + \mathrm{jTz}^3, \quad (1)$$

where SS is sound speed (m/s), T is temperature (°C), S is salinity and z is depth (m). Coefficients are: $a = 1448.96$ m s^{-1}, $b = 4.591$ m s^{-1} C^{-1}, $c = -5.304{\cdot}10^{-2}$ m s^{-1} C^{-2}, $d = 2.374{\cdot}10^{-4}$ m s^{-1} C^{-3}, $e = 1.340$ m s^{-1}, $f = 1.630{\cdot}10^{-2}$ s^{-1}, $g = 1.675{\cdot}10^{-7}$ m^{-1} s^{-1}, $h = -1.025{\cdot}10^{-2}$ m s^{-1} C^{-1}, $j = -7.139{\cdot}10^{-13}$ m^{-2} s^{-1} C^{-1}.

The Mackenzie formula exploits the link between temperature, salinity, depth, and sound speed. It is a nine-term, eight-variable equation to compute sound speed in the ocean, valid in a range of temperature between −2° and 30°C, salinity 25–40 psu, depth 0–8,000 m. The formula stems from data gathered at 15 worldwide stations and calculations of sound speeds for each pressure. We computed sound speed for all months of each data set; then, we extracted the monthly averages over the present and future decades. In order to quantify the seasonal variability, we also computed the annual standard deviation (STD) from the 12 monthly averages. Using the uncertainty estimates of salinity and temperature, $\Delta S(z)$ and $\Delta T(z)$, derived by the technical documentation of the original data sets (see Table 2), we estimated the sound speed uncertainty ΔSS (T,S,z), following Salon et al. (2003) and safely neglecting the contribution of the depth uncertainty:

$$\Delta\mathrm{SS}(T,S,z) = \left(b + 2\mathrm{cT} + 3\mathrm{d}T^2 + h(S-35) + \mathrm{jz}^3\right)\Delta T(z) + (e + \mathrm{hT})\Delta S(z). \quad (2)$$

The computation of the SS uncertainty is essential to estimate its magnitude in comparison to both the mean seasonal variation (mainly in the upper ocean layer) and the expected climatic signal, considering that SS, at the first order of the MacKenzie formula, linearly increases with the temperature:

$$\mathrm{SS}(T,S,z) = a + \left(b + h(S-35) + \mathrm{jz}^3\right)T + O\left(T^2\right). \quad (3)$$

The SS uncertainty is maximum for the LENS scenario data sets (about 6 m/s at 50 m in the polar areas, see Figure S1 in Supporting Information S1), but is not uniform in the global ocean, thus setting a regional reference threshold for the climatic signal, as discussed in Section 3.1.

2.3. Expected Sound Speed Changes and Identification of "Acoustic Hotpots"

SS climate change was estimated by comparing the SS fields calculated for the LENS present and future decades considered (i.e., LENS-pres and LENS-futr). In order to assess the LENS reconstruction of the present state and demonstrate a reliable representation of current SS conditions we compared the decade 2005–2015 of REAN data sets with the LENS-pres climate scenario for 2006–2016. Then, we performed a quantitative comparison between the two LENS decades (i.e., LENS-futr minus LENS-pres), which share the same computational grid (Table 1), by calculating the difference of SS for each of the 60 vertical levels and for each grid cell. The calculation allowed us to estimate the expected variations due to the selected climate change scenario at global scale.

Seasonal SS variations were also calculated for the months that represent the boreal winter and summer extreme conditions (March and September, respectively). Based on that, we produced vertical sections for March and September on a global scale and for selected meridians (see Figure S2 in Supporting Information S1).

Based on the computed sound speed variations, we identified climate-induced acoustic hotspots where changes larger than 1.5% are expected at both shallow and deep layers, identified at 50 and 500 m depth respectively. Only the areas where the climatic signal was greater than the seasonal signal were selected. The seasonal signal was expressed by the STD, which was computed from the 12 SS monthly averages (see Section 2.2 for details). For each identified area, we extracted the vertical average profiles of temperature, salinity, and sound speed.

2.4. Transmission Loss and Sample Species Selection

To quantify the effect on the sound propagation, we investigated the sound transmission loss (TL) for present and future scenarios in one of the two selected acoustic hotspots (identified as described in Section 2.3). The calculation is based on the present and future vertical profiles of temperature and salinity and the computed sound speed (in the layer 0–5,000 m) obtained from the LENS-pres and LENS-futr data sets. The density profile has been computed from the values of temperature and salinity using the Gibbs-Sea Water Oceanographic Toolbox-TEOS-10 (http://www.teos-10.org/pubs/gsw/html/gsw_contents.html). The bathymetry was chosen inside the selected area using GEBCO-The General Bathymetric Chart of the Oceans (https://download.gebco.net). TL was computed using ray tracing (this technique can also be used for low-frequency, as demonstrated by Hovem & Dong, 2019) using 350 rays at an angle of 30°.

In order to carry out this example, we chose as a sample species, the North Atlantic right whale (*Eubalaena glacialis*), also referred to as NARW. These whales are listed as Critically Endangered by IUCN 3.1 (Cooke, 2020) and more information and data need to be collected in order to develop an effective strategy (Meyer-Gutbrod &Greene, 2018). Moreover, NARWs are present in the area we chose to study for this example, the north-western Atlantic Ocean. We considered a potential acoustic communication between two NARWs. In this case, these animals act as a source producing the stereotypical "up-calls" vocalizing at 50 Hz and placed at 50 m depth.

3. Results

3.1. Global Sound Speed in Present Decade

For each data set described in Section 2.1, we produced global maps of sound speed and associated uncertainty at different depths. The sound speed calculation was based on the procedure described in Section 2.2. Figure 1 shows the mean SS fields for the present decade for REAN and LENS-pres, and their associated STD, at two selected depths (50 and 500 m, respectively). Plots of annual mean sound speed uncertainty (also referred as "error") for the REAN and LENS-pres data sets are provided in Supporting Information S1 (Figure S1).

At 50 m depth, the global field of SS in the REAN data set is characterized by a meridional gradient (Figure 1a), closely related to the thermohaline properties, with values lower than 1,450 m/s in the polar areas, increasing to over 1,530 m/s in the equatorial band. The effect of the Gulf Stream (SS values around 1,480 m/s) is clearly visible in the northern Atlantic Ocean. The seasonal variation of SS in the REAN data set (Figure 1c), quantified by the annual STD, is generally below 6 m/s, only reaching 10–12 m/s in the areas most affected by substantial seasonal variations of temperature and salinity: Gulf Stream, Kuroshio, and the eastern flank of the Northern Equatorial Current that interacts with the southern part of the California Current. The SS error, a measure of the SS field computation uncertainty (included in Supporting Information S1; Figure S1), reaches 3.4 m/s at the poles. Its annual variation (not shown) is one order of magnitude lower and can be safely neglected. The LENS-pres data set (Figure 1b) reproduces the main features of the global SS field described for REAN (Figure 1a), although the LENS-pres SS field appears smoother, also due to the coarser resolution, and with weaker gradients (see, for example, the area of Gulf Stream in the north-western Atlantic). These differences were also observed for the seasonal cycle. The mean SS error in LENS-pres reaches 6 m/s in the polar areas (Figure S1 in Supporting Information S1), with a maximum variation of 0.4 m/s (not shown).

At 500 m (Figure 1e), REAN SS gradients are, in general, less strong apart from a few regions (e.g., north-western Atlantic), and the global field ranges between 1,450 and 1,520 m/s, except areas as the Mediterranean Sea and the western Sargasso Sea. Similarly to what is described at 50 m depth, there is a fair agreement for annual mean SS between REAN and LENS-pres (Figures 1e and 1f). In addition, REAN SS seasonal variability (quantified by the STD of SS, Figure 1g) is mostly below 1 m/s, except for a few areas where it reaches 4 m/s, among the others the Kuroshio and the Gulf Stream detachments, the Arctic Ocean north of the Svalbard Archipelago. At 500 m the LENS-pres scenario has a mean SS error (Figure S1 in Supporting Information S1) reaching 5.4 m/s in the polar areas.

3.2. Seasonal Sound Speed Variations

Figure 2 shows the mean global vertical sections for March and September, as computed in the LENS present scenario, and the difference with the future projection. Vertical sections at three selected longitudes (10°, 30°W

10.1029/2021EF002099

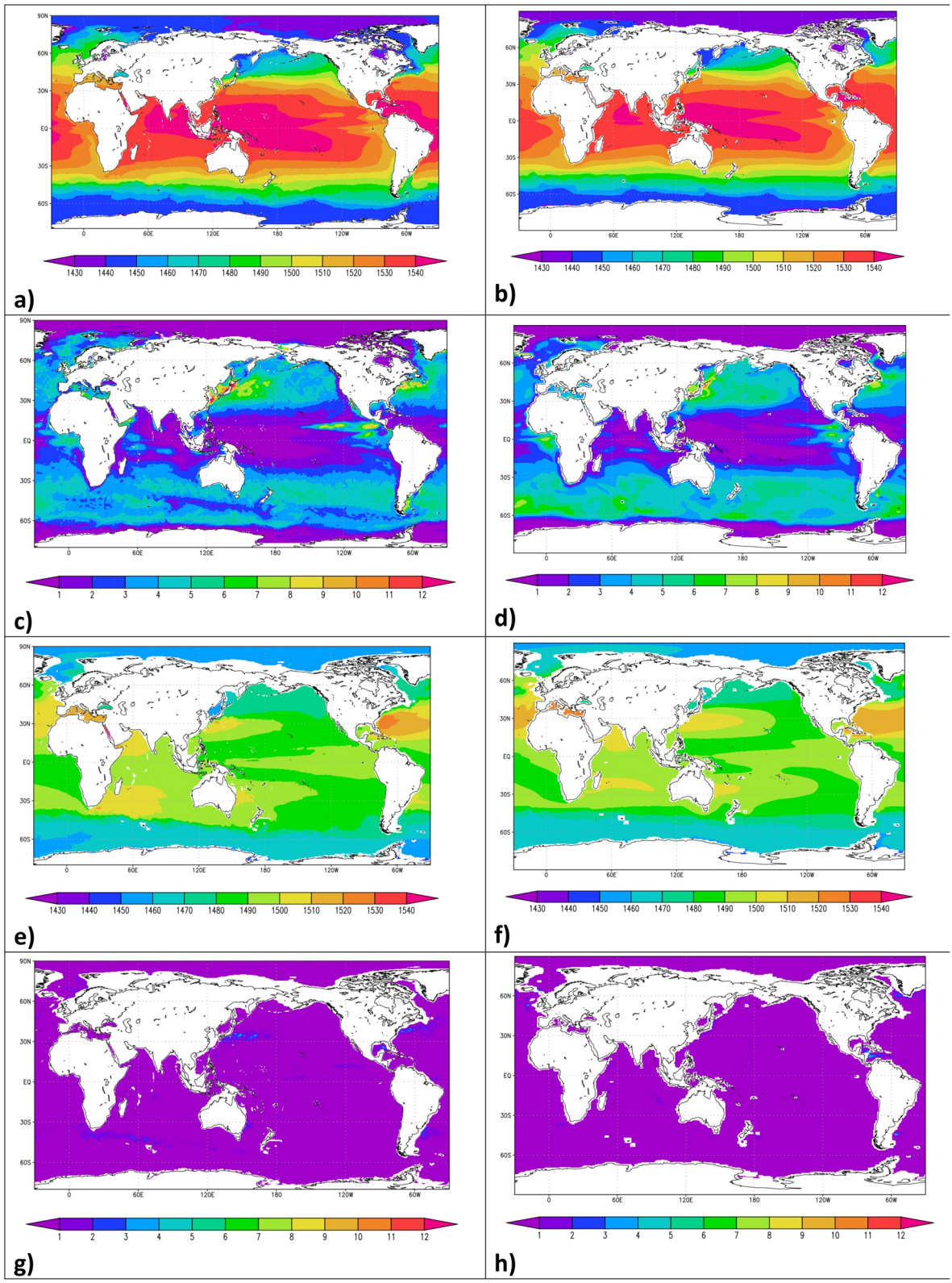

Figure 1. Global sound speed annual mean and standard deviation maps for REAN and LENS-PRES data sets (left and right column, respectively) at (a)–(d) 50 m and (e)–(h) 500 m.

10.1029/2021EF002099

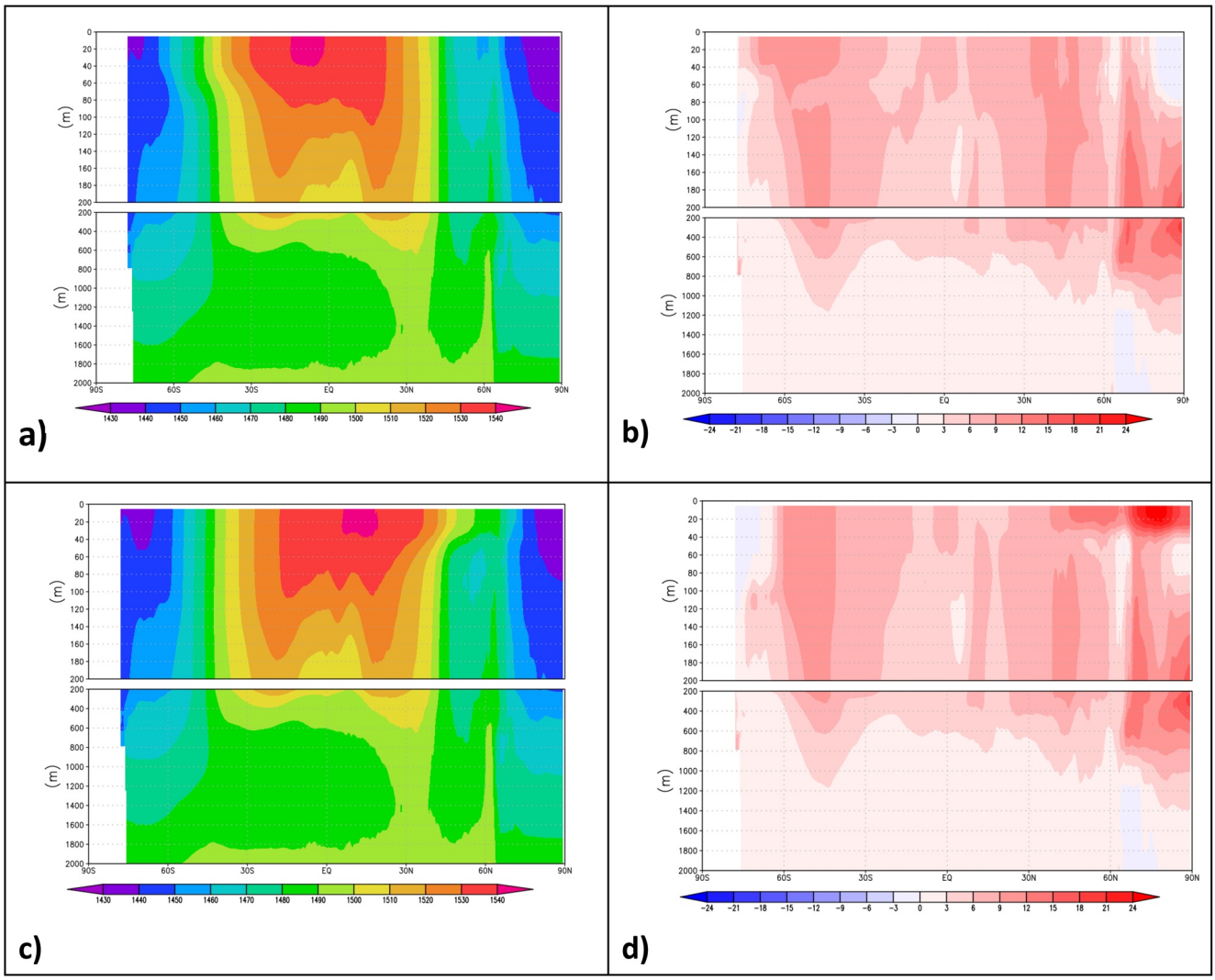

Figure 2. Left panels: Global meridional section of sound speed means (0–2,000 m) in March and September for the LENS-PRES data set and right panels: the difference future–present. Note that the vertical scale is finer (20 m) in the upper layer, in order to grasp the greater changes expected at the shallow layers, while it is coarser (200 m) at the deeper layers.

and 180°E) are included in Supporting Information S1 (Figures S2–S4). The upper layer (0–200 m) shows a seasonal cycle of the SS vertical profile with a meridional displacement of the near-equatorial maximum value (larger than 1,540 m/s) from March to September, a monotonic increasing profile in the polar areas, and a clear signature of the permanent minimum value (between 1,480 and 1,490 m/s) in the layer 1,200–1,400 m, identified as the SOFAR channel (Dashen et al., 2010; Munk et al., 1995; Northrop & Colborn, 1974; Wagstaff, 1981). As already seen at 50 and 500 m depth, the climate signal (Figures 2b and 2d) is particularly intense in the northern polar areas (latitudes north of 60°N), with SS increments larger than 24 m/s in September in the surface layer and more than 15 m/s in the layer 200–500 m: at these depths, most marine mammals perform important biological activities. The signal reaches differences even more considerable along the transect at 10°W (see Figure S2 in Supporting Information S1 for details). At deeper levels, differences remain limited to 5 m/s, a value lower than or at the same order of the model error, thus preventing any considerations concerning the climate change effect.

3.3. Future Global SS Variations and Selected "Acoustic Hotspots"

Based on the SS fields calculated for present (shown in Figure 1) and future decades by the LENS model system, we computed the SS variations at 50 and 500 m depth, shown as relative differences with respect to the present

10.1029/2021EF002099

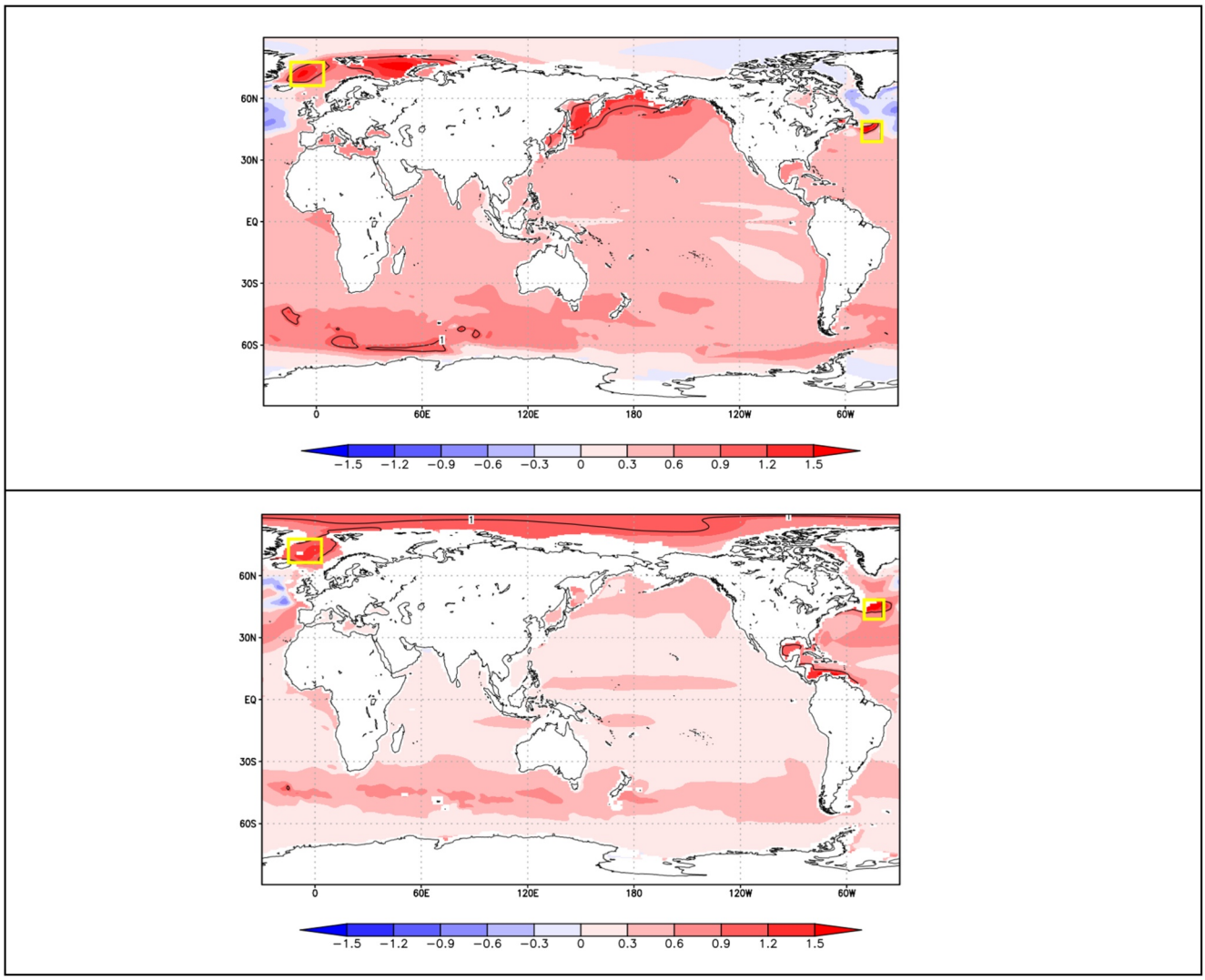

Figure 3. Relative % sound speed difference between future and present LENS scenarios at 50 and 500 m depth. The contour line identifies the threshold of 1% difference. The yellow rectangles in the Greenland sea and the north-western Atlantic Ocean-Newfoundland shelf identify the selected acoustic hotspots, where sound speed variations exceed the 1.5%. Absolute difference maps are in Supporting Information S1 (Figure S5).

conditions (Figure 3; the absolute difference maps are in Figure S5 in Supporting Information S1). The mean SS field in LENS-futr appears to generally increase, as shown by the general positive SS differences values. At 50 m, a larger intertropical area characterized by increments between 5 and 10 m/s and a visible poleward expansion of the higher values are observed (Arctic Sea, northern Pacific, and the Southern Ocean have differences larger than 10 m/s; Figure S5 in Supporting Information S1). The only area which shows a decrease of the mean annual SS (up to −10 m/s) is the Labrador Sea and the northern Atlantic, which may be related to a shift in the Gulf Stream fronts in this region, potentially changing the sound propagation (Lynch et al., 2018). Major SS variations are found in the northern Pacific Ocean, in the western Arctic (Norwegian and Barents seas), and in the Southern Ocean. A strong signal (larger than 30 m/s) is observable in September near the Labrador's current southern flanks (not shown), somehow balanced by a decrease in the northern Atlantic. In most of the polar areas, differences are lower than the SS uncertainty for the LENS model (Figure S1 in Supporting Information S1), so we cannot relate it to climate change. The analysis of the climate signal at 500 m is somehow similar to what already described at 50 m: Figure 3 (bottom panel) shows that a general increment of SS is also projected at intermediate depth, with relative difference larger than 1% in the whole Arctic Ocean, north-western and north-eastern Atlantic, Gulf of Mexico, southern Caribbean Sea (differences larger than 10 m/s, Figure S5 in Supporting Information S1). The midlatitude portion of the Atlantic west of the shelf is the only region characterized by a negative

difference larger than −5 m/s. The climatic signal is larger than seasonal variability over the upper 1,000 m layer, specifically at latitudes higher than 60°N (reaching up to 20 m/s in September, Figure 2). Deeper layers, which are not affected by seasonal variability, show nonetheless a climatic signal that can cause SS variations larger than 1%, roughly corresponding to 15 m/s.

The areas with greater SS variation are the Greenland Sea, with a mean annual increase in SS higher than 1%, corresponding to more than 15 m/s (Figure S5 in Supporting Information S1), almost three times larger than the model error estimated in the Polar regions. We also observe an increment larger than 1% in the north-western Atlantic, increasing to more than 20 m/s (Figure S5 in Supporting Information S1) in the Labrador's current southern flanks, east to Newfoundland. Areas impacted by climatic variations larger than 1% can be observed in the north-western Pacific Ocean and in the Southern Ocean between 0° and 60°E, though this difference is much lower at 500 m (roughly around 0.5%).

We can thus identify two "acoustic hotspots" where sound speed variations greater than 1.5% (which corresponds to approximately 25 m/s) are expected at both shallow and deep layers (see Figure 3). The selected areas are the Greenland Sea and the north-western Atlantic Ocean-Newfoundland shelf (so on called "greenland" and "nwatl," respectively). For these areas, the climatic signal is greater than the seasonal signal and exceeds the model uncertainty at both shallow and deep layers. Note that the seasonal variation at 500 m (Figures 1g and 1h) is almost null so the expected SS variation can be entirely associated with climate change.

3.4. Sound Speed Variation in the "Acoustic Hotposts"

Figure 4 shows the average vertical profiles of temperature, salinity and sound speed computed for the two identified "acoustic hotspots", greenland and nwatl, in the first 2000 m depth. Profiles are shown for the present and the future scenarios (LENS-pres and LENS-futr data sets). The SS vertical profiles are associated with their seasonal variability (estimated by the annual STD and model error (ERR). Figure 4 shows that, in the future, a positive sound velocity gradient is expected in the mixed layer and at deeper levels in nwatl. The figure shows the presence of the surface duct and the deep SOFAR channel, which is shallower in greenland and deeper and wider in nwatl. A clear relation is visible between the temperature and SS variation, in particular above the deep sound channel axis. The SS decreases with depth due to the decrease in temperature through the thermocline. Below the deep sound channel axis, the temperature is practically constant, and following the pressure increase, the sound speed increases with depth. This situation leads to a scenario where sound waves above the deep sound channel axis refract toward the sea bottom. At the same time, those below the deep sound channel axis refract toward the surface.

3.5. Expected Variations in Sound Transmission Loss

The TL was investigated for the North Atlantic right whale (*Eubalaena glacialis*), which lives in both acoustic hotspots previously identified, and is considered Critically Endangered (IUCN 3.1) and protected under the U.S. Endangered Species Act and Marine Mammal Protection Act and the Canada's Species at Risk Act (Cooke, 2020). These whales produce a common vocalization known as "upcall" that ranges from 50 to 350 Hz (Clark et al., 2007). The lower value, 50 Hz, was used as the source frequency and 170 dB ref 1 Pa at 1 m as source level (Johnson & Tyack, 2003). We hypothesized that the source frequency of the whale call would be constant over the next 100 years because we do not have any other means to assess its future variation. The source was placed at a depth of 50 m depth since these whales live in the first 100 m of the ocean (https://www.hww.ca/en/wildlife/mammals/North-Atlantic-Right-Whale.html).

Figure 5 shows the ray tracing propagation for the nwatl area for the present (top) and the future (bottom) scenario. The plot includes only rays with TL < 130 dB and shows the reflected and refracted rays. In the ray trace plots in Figure 5 the very high transmission losses occur in regions where there are no rays or a low density of rays. Results for the future scenario show that sound waves form a surface duct, depending on the steepness of the sound speed gradient or the considered frequency. The sound waves are reflected upwards and downwards depending on the interactions with the bottom and the surface. The greater the sound speed gradient, the more the sound waves curve. Sound will always refract toward a depth with a lower sound speed. With a 30° angle for rays to depart from the source, these rays look steep enough to refract back to the surface. Shallower ray paths remain in the duct, but steeper rays refract toward the bottom, meeting the negative sound speed gradient. The formation

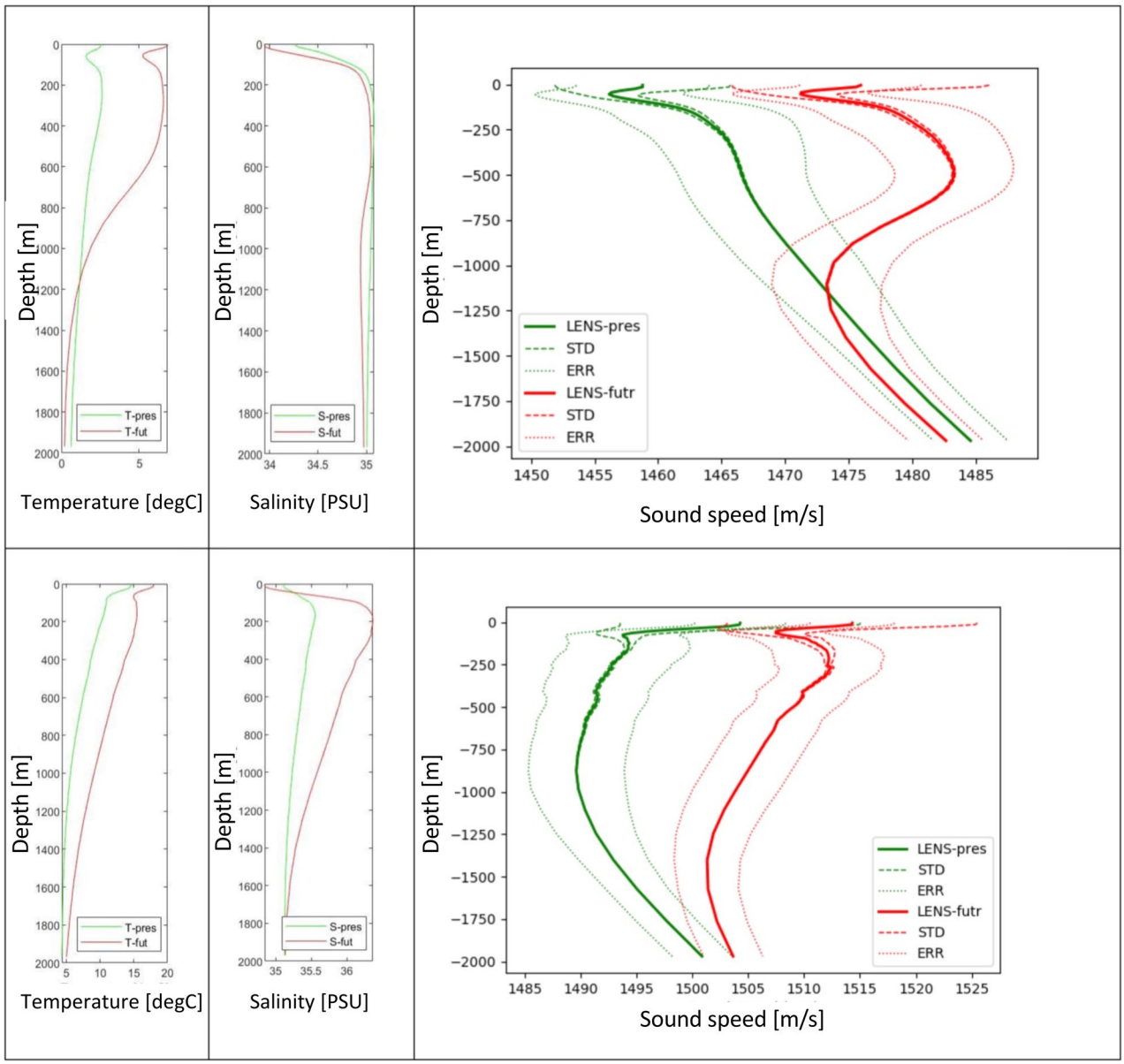

Figure 4. Average temperature, salinity, and sound speed vertical profiles (from left, to right, respectively) from surface to 2,000 m depth for the two acoustic hotspots (greenland and nwatl) extracted from the Community Earth System Model Large Ensemble project (LENS)-pres scenario (green solid lines) and the LENS-futr (red solid lines), with corresponding standard deviations (light dashed line) and errors (light dotted lines).

of the surface duct is consistent with the future temperature profile. Apart from the duct, the other significant differences between present and future scenarios are found at larger distances.

Figure 6 shows the results of TL computation at 50 m, the same depth of the source. In our example, we consider a scenario where one whale could communicate with another at the same depth. The plot shows that TL in the future (red line, LENS-futr) diminishes, leading to a potential increase in sound propagation.

4. Discussion

In this work, we produced a global ocean sound speed data set based on the RCP8.5 scenario at the end of XXI century, and computed the differences with the present conditions. Results highlighted that sound speed is projected to increase at a global scale (Figures 2 and 3) and allowed the identification of the areas where

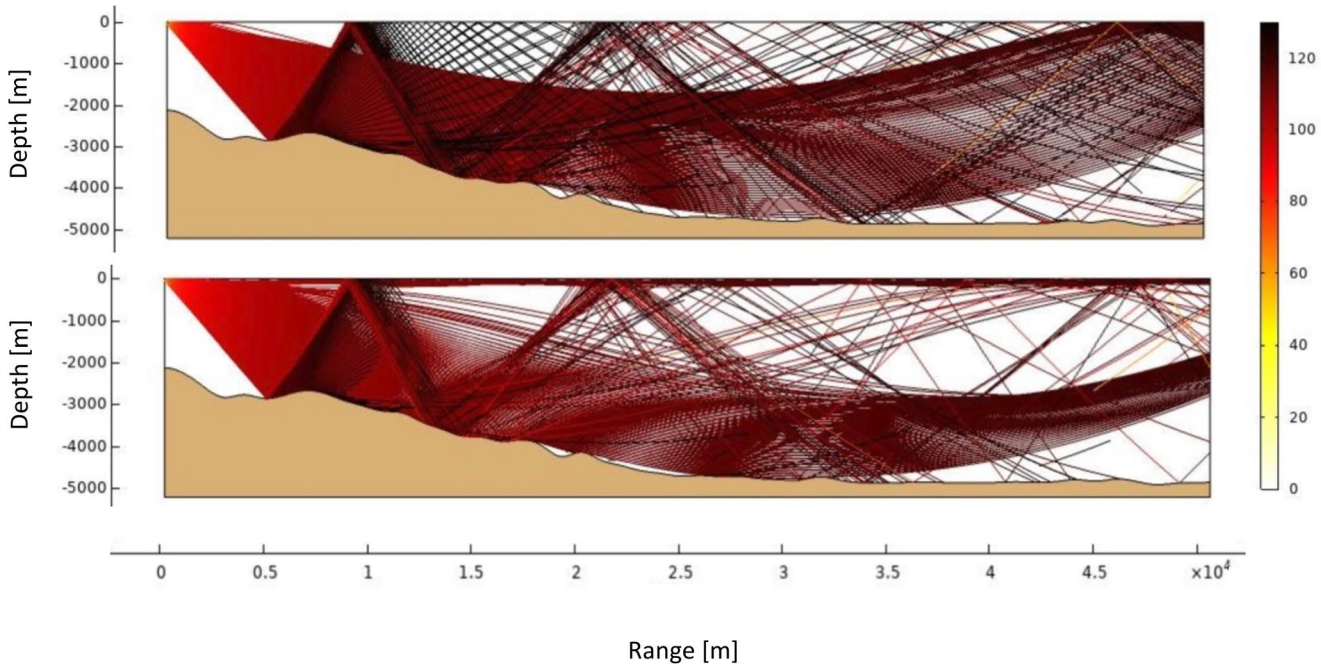

Figure 5. Case study for the North Atlantic right whale: (top panel) transmission loss [dB] in the nwatl acoustic hotspot for the present and (lower panel) the future scenario.

the climatic signal is significant, that is, it is larger than the seasonal variability and the model uncertainty. We selected two areas, called acoustic hotspots, with the largest SS variations (i.e., where the relative difference between future and present has SS values larger than 1.5%) at 50 and 500 m depths. These two depth levels are used as proxies for upper and deeper layers.

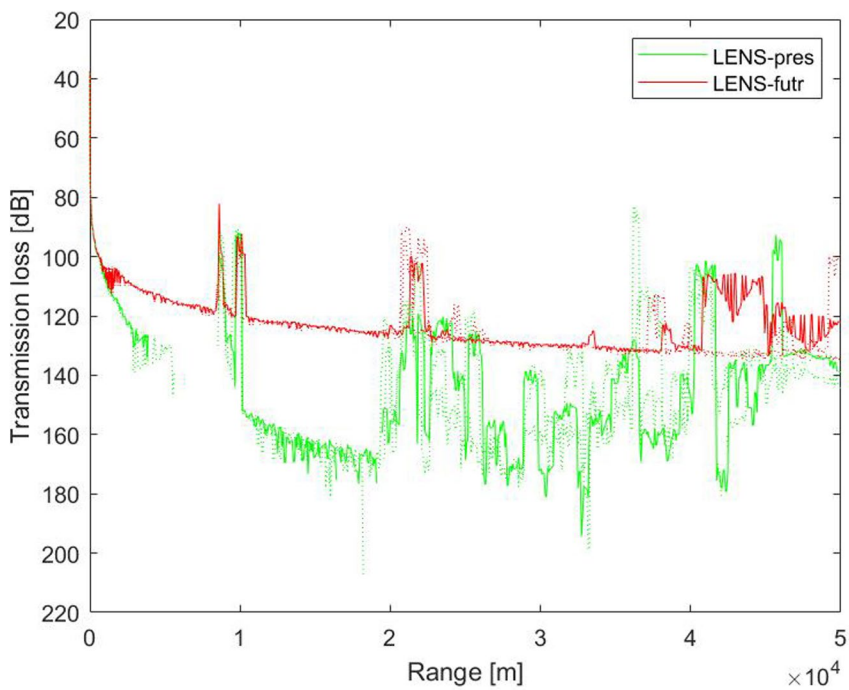

Figure 6. Transmission loss in the nwatl acoustic hotspot (at 50 m) for the present (in green) and future scenarios (in red) with uncertainties (dotted lines). For clarity, the uncertainty range is computed considering the mean sound speed at 50 m and adding/subtracting the related value of the error at the same depth.

In Figure 4, the nwatl LENS-pres sound speed profile follows a deep-water profile typical of midlatitudes with the addition of a small sound speed minimum at about 100 m depth. The other significant feature is the minimum in the sound speed at a depth of about 900 m, which results in the SOFAR channel. The source plays a different role depending on its depth: sound from a source at 50 m depth is refracted down and upward by the sound speed gradient. It goes through convergence zone propagation patterns, at intervals of about 45 km (Figure 5). Two North Atlantic right whales at 50 m depth would be able to communicate at ranges of one or two km, before encountering a shadow zone (Figure 5). Looking at the LENS-futr sound speed profile (Figure 4), we see a strong minimum at a depth of approximately 100 m, which allows the constriction of sound to a narrow depth range and a propagation through a surface duct. This duct allows a more reliable communication, with respect to the present conditions, between two whales at a depth of 50 m. There is no interaction with the sea surface or bottom, and low losses. There is a deep sound channel axis at about 1,400 m, which changes the geometry of the convergence zone propagation.

Following the work by Hovem and Dong (2019) we used the ray tracing technique to plot TL for one of the chosen acoustic hotspots (nwatl): this led us to observe that the sound propagation in this specific area will change, leading to a different value of TL by the end of the century. Here we considered a specific example either in terms of selected area, frequency, and TL computation technique, providing evidence that TL will vary in the future, affecting underwater sound propagation. Future work should explore the TL computation under different computation methods and input parameters (e.g., source depth, source level, and bathymetry).

In 2009, McDonald et al. (2009) analyzed the evolution of Blue whale (*Balaenoptera musculus*) songs from the 1960s, finding out that their frequencies had shifted downward in time, becoming 31% lower. In that case, the authors' thesis suggests that this shift was due to a decrease in population number due to whaling. The animals were lower in number and their vocalizations had more space to cover before reaching the closest individual. Therefore, they adjusted their frequency accordingly. Although our study looks at a different variable, we ask ourselves if a similar situation might happen in the future. Since sound is projected to be far ranging faster, will the whales shift their frequencies in order to exploit this situation?

Furthermore, it is worth considering that sound produced by anthropogenic sources will also propagate faster, potentially leading to problematic consequences for acoustic pollution. Anthropogenic sources are constantly growing (Duarte et al., 2021) and likely to increase in the future, changing the soundscape. In addition, soundscape might undergo strong variations also due to changes in current patterns or geophysical events (e.g., Miksis-Olds et al., 2018), though the impact of such changes on marine life has been so far poorly investigated.

In this paper we provide a global data set that could be exploited and adapted to specific areas and species in future works, thus supporting the assessment of climate change impacts. Even though the increase in ocean temperature impacts deep and abyssal layers (Desbruyères et al., 2016), thus directly affecting the vertical profile of SS, most studies are focused on the surface. However, a global, three-dimensional view of the ocean is particularly relevant, also from a biological point of view, because some marine mammals, such as sperm whales, carry out vital functions both at the surface and deep layers (Heidemann et al., 2012). The results displayed in this study cover all ocean depths; therefore, they take into consideration the vulnerability of these deep divers and provide a starting point for three-dimensional expected changes in the speed of the propagation of the acoustic field (Figures 4 and 5).

The selected acoustic hotspots here investigated have been already indicated as problematic by other works. For example, Halpern et al. (2008) define global cumulative anthropogenic impacts, and categorize the selected hotspots as "medium-high impact." Despite the study dates back to 2008, we do not expect the situation to have improved. The overlapping of the acoustic hotspot with an area that is already threatened by anthropogenic pressures might lead to cumulative and synergistic effects which, in the field of underwater acoustics, are still under investigation. Expected changes in SS propagation should be also taken into account when developing ocean management plans in order to minimize the impacts on marine fauna. Studies such as the one presented here may help identify the particular vulnerability of some areas where these changes are substantial and where specific monitoring efforts should be carried out or instrumentation should be deployed.

5. Conclusions and Outlook

In this work, we investigated future sound speed changes under the RCP8.5 climate scenario. We produced a three-dimensional global sound speed data set that allows assessing the expected sound speed changes at multiple depths. We identified two areas of interest ("acoustic hotspots") where we expect significant SS changes both in superficial and deeper layers by the end of the century. Having quantified the sound speed variations in each target area and for multiple depth levels, we found that climate-change-induced sound speed variations are substantial, reaching up to 1.5% (approximately 20 m/s) and exceeding the SS seasonal variability. Based on the quantified changes, we assessed the impact of SS variation on the sound propagation for a selected endangered species living in the acoustic hotspot located in the north-western Atlantic Ocean, showing that the transmission loss can vary in future.

Our results shed some light on the particular aspect of sound propagation, which could contribute to the impending risk of biodiversity loss at global scale. The sound speed variation data set and the profiles produced here show how sound speed is expected to vary in the future and can serve as strong support for multidisciplinary, interdisciplinary, and transdisciplinary studies focused on the interactions between oceanography, climate sciences, and marine biology. The provided data set puts the basis for further research on the role of anthropogenic noise in emphasizing the ongoing climate-change impact on marine mammal's communication.

Mitigating the anthropogenic impact on the ocean is a challenge that should rely on quantitative and qualitative information and involve the participation of a wide range of stakeholders, from policy-makers to the scientific community, to practitioners, to public and private actors, and the representatives of civil society (Foley et al., 2020). Future efforts should, of course, be coordinated and aligned with the ongoing strategies (e.g., the Sustainable Development Goals, or the European Blue Growth strategy) that promote the monitoring, conservation, and preservation of biodiversity and pursue the common goal of improving human health through the responsible use of the ecosystem services the ocean can provide.

Acknowledgments
This study has been conducted based on the data sets provided by the European Copernicus Marine Environment Monitoring Service (CMEMS) and the U.S. National Center for Atmospheric Research (NCAR/UCAR). The authors acknowledge Elena di Medio (CMEMS Service Desk) for the great support provided in downloading the data at global scale for multiple decades. The authors also thank Adam Phillips (Climate and Global Dynamics Laboratory, NCAR) and Eric Niehouse (Software Applications & Gateway Engineering, NCAR) for their clarification on the available data sets and the retrieval options. Funding for this study has been provided by the National Institute of Oceanography and Applied Geophysics-OGS within the Blue Growth activities supported by the Ministry of University and Research (MUR). Chiara Scaini is partially supported by OGS and CINECA under HPC-TRES program award number 2019-03. Data processing and analysis was carried out at the CINECA facility (Bologna, Italy). The authors sincerely thank Angelo Camerlenghi, Stefano Parolai, and Cosimo Solidoro for critically reading this manuscript, providing helpful comments and suggestions. The reviewers are gratefully acknowledged for their comments and suggestions which contributed significantly to an improved version of the manuscript.

Data Availability Statement

Sound speed data are available from the NOAA National Centers for Environmental Information (NCEI), FAIR-compliant repository at https://www.ncei.noaa.gov/archive/accession/0244993. All the data used are described in the manuscript and in Supporting Information S1. Global Ocean Physics Reanalysis (GLORYS2V4) from the catalog of the European Copernicus Marine Environment Monitoring Service (CMEMS; referred to as "REAN" in the manuscript): https://resources.marine.copernicus.eu/?option=com_csw&view=details&product_id=GLOBAL_REANALYSIS_PHY_001_031. Note that for the analysis we used the previous version of this data set (see Supporting Information S1 for details). Community Earth System Model (CESM) Large Ensemble (LENS) Community Project (referred to as "LENS" in the manuscript): https://www.cesm.ucar.edu/projects/community-projects/LENS/data-sets.html. The technical documentation for the data set is available at: www.cesm.ucar.edu/experiments/cesm1.1/LE/diagnostics/ens001/ocn_1981-2005-obs/popdiag.html.

References

Albouy, C., Delattre, V., Donati, G., Frölicher, T. L., Albouy-Boyer, S., Rufino, M., & Leprieur, F. (2020). Global vulnerability of marine mammals to global warming. *Scientific Reports*, *10*(1), 1–12. https://doi.org/10.1038/s41598-019-57280-3

Au, W. W., & Hastings, M. C. (2008). *Principles of marine bioacoustics* (Vol. 510). Springer.

Clark, C. W., Gillespie, D., Nowacek, D. P., Parks, S. E., Kraus, S. D., & Rolland, R. M. (2007). Listening to their world: Acoustics for monitoring and protecting right whales in an urbanized ocean. In *The urban whale: North Atlantic right whales at the crossroads* (pp. 333–357). Harvard University Press.

Cooke, J. G. (2020). *Eubalaena glacialis. The IUCN red list of threatened species 2020:e.T41712A162001243*. (accessed 28 March 2021). https://doi.org/10.2305/IUCN.UK.2020-2.RLTS.T41712A162001243.en

Dashen, R., Munk, W. H., Watson, K. M., & Zachariasen, F. (2010). *Sound transmission through a fluctuating ocean*. Cambridge University Press.

Desbruyères, D. G., Purkey, S. G., McDonagh, E. L., Johnson, G. C., & King, B. A. (2016). Deep and abyssal ocean warming from 35 years of repeat hydrography. *Geophysical Research Letters*, *43*(19), 10356–10365. https://doi.org/10.1002/2016GL070413

Doney, S. C., Ruckelshaus, M., Emmett Duffy, J., Barry, J. P., Chan, F., English, C. A., & Talley, L. D. (2012). Climate change impacts on marine ecosystems. *Annual Review of Marine Science*, *4*, 11–37. https://doi.org/10.1146/annurev-marine-041911-111611

Duarte, C. M., Agusti, S., Barbier, E., Britten, G. L., Castilla, J. C., Gattuso, J. P., et al. (2020). Rebuilding marine life. *Nature*, *580*(7801), 39–51. https://doi.org/10.1038/s41586-020-2146-7

Duarte, C. M., Chapuis, L., Collin, S. P., Costa, D. P., Devassy, R. P., Eguiluz, V. M., et al. (2021). The soundscape of the Anthropocene ocean. *Science*, *371*(6529), eaba4658. https://doi.org/10.1126/science.aba4658

Dushaw, B. D., Worcester, P. F., Cornuelle, B. D., & Howe, B. M. (1993). On equations for the speed of sound in seawater. *Journal of the Acoustical Society of America*, *93*(1), 255–275. https://doi.org/10.1121/1.405660

Foley, P., Pinkerton, E., Wiber, M., & Stephenson, R. (2020). Full-spectrum sustainability: An alternative to fisheries management panaceas. *Ecology and Society*, *25*(2). https://doi.org/10.5751/ES-11509-250201

GEF LME:LEARN. (2017). *The Large marine ecosystem Approach: An engine for achieving SDG 14*.

Global Monitoring and Forecasting Center. (2018). *GLORYS2V4 - Global Ocean Physical Reanalysis Product, E.U. Copernicus Marine Service Information [PHY_001_025]. Replaced by GLOBAL_REANALYSIS_PHY_001_031*. Retrieved March 2020, from https://resources.marine.copernicus.eu/product-detail/GLOBAL_REANALYSIS_PHY_001_031/INFORMATION

Halpern, B. S., Walbridge, S., Selkoe, K. A., Kappel, C. V., Micheli, F., D'Agrosa, C., & Watson, R. (2008). A global map of human impact on marine ecosystems. *Science*, *319*(5865), 948–952. https://doi.org/10.1126/science.1149345

Heidemann, J., Stojanovic, M., & Zorzi, M. (2012). Underwater sensor networks: Applications, advances and challenges. *Philosophical Transactions of the Royal Society A: Mathematical, Physical & Engineering Sciences*, *370*, 158–175. https://doi.org/10.1098/rsta.2011.0214

Hildebrand, J. A. (2009). Anthropogenic and natural sources of ambient noise in the ocean. *Marine Ecology Progress Series*, *395*, 5–20. https://doi.org/10.3354/meps08353

Hoegh-Guldberg, O., & Bruno, J. F. (2010). The impact of climate change on the world's marine ecosystems. *Science*, *328*(5985), 1523–1528. https://doi.org/10.1126/science.1189930

Hovem, J. M., & Dong, H. (2019). Understanding ocean acoustics by eigenray analysis. *Journal of Marine Science and Engineering*, *7*(4), 118. https://doi.org/10.3390/jmse7040118

Johnson, G. C., & Lyman, J. M. (2020). Warming trends increasingly dominate global ocean. *Nature Climate Change*, *10*(8), 757–761. https://doi.org/10.1038/s41558-020-0822-0

Johnson, M. P., & Tyack, P. L. (2003). A digital acoustic recording tag for measuring the response of wild marine mammals to sound. *IEEE Journal of Oceanic Engineering*, *28*(1), 3–12. https://doi.org/10.1109/joe.2002.808212

Kay, J. E., Deser, C., Phillips, A., Mai, A., Hannay, C., Strand, G., et al. (2015). The community Earth system model (CESM) large ensemble project: A community resource for studying climate change in the presence of internal climate variability. *Bulletin of the American Meteorological Society*, *96*(8), 1333–1349. https://doi.org/10.1175/bams-d-13-00255.1

Lynch, J. F., Gawarkiewicz, G. G., Lin, Y. T., Duda, T. F., & Newhall, A. E. (2018). Impacts of ocean warming on acoustic propagation over continental shelf and slope regions. *Oceanography*, *31*(2), 174–181. https://doi.org/10.5670/oceanog.2018.219

Mackenzie, K. V. (1981). Nine-term equation for sound speed in the oceans. *Journal of the Acoustical Society of America*, *70*(3), 807–812. https://doi.org/10.1121/1.386920

McDonald, M. A., Hildebrand, J. A., & Mesnick, S. (2009). Worldwide decline in tonal frequencies of blue whale songs. *Endangered Species Research*, *9*(1), 13–21. https://doi.org/10.3354/esr00217

Meyer-Gutbrod, E. L., & Greene, C. H. (2018). Uncertain recovery of the North Atlantic right whale in a changing ocean. *Global Change Biology*, *24*(1), 455–464. https://doi.org/10.1111/gcb.13929

Miksis-Olds, J. L., Martin, B., & Tyack, P. L. (2018). Exploring the ocean through soundscapes. *Acoustics Today*, *14*, 26–34.

Munk, W., Worcester, P., & Wunsch, C. (1995). *Ocean acoustic tomography*. Cambridge University Press.

Northrop, J., & Colborn, J. G. (1974). Sofar channel axial sound speed and depth in the Atlantic Ocean. *Journal of Geophysical Research*, *79*(36), 5633–5641. https://doi.org/10.1029/JC079i036p05633

Reser, J. P., & Swim, J. K. (2011). Adapting to and coping with the threat and impacts of climate change. *American Psychologist*, *66*(4), 277–289. https://doi.org/10.1037/a0023412

Salon, S., Crise, A., Picco, P., Marinis, E. D., & Gasparini, O. (2003). Sound speed in the Mediterranean Sea: An analysis from a climatological data set. *Annales Geophysicae*, *21*(3), 833–846. https://doi.org/10.5194/angeo-21-833-2003

Schulzweida, U. (2019). *CDO user guide*. Version 1.9.8. https://doi.org/10.5281/zenodo.3539275

Tittensor, D. P., Mora, C., Jetz, W., Lotze, H. K., Ricard, D., Berghe, E. V., & Worm, B. (2010). Global patterns and predictors of marine biodiversity across taxa. *Nature*, *466*(7310), 1098–1101. https://doi.org/10.1038/nature09329

Trisos, C. H., Merow, C., & Pigot, A. L. (2020). The projected timing of abrupt ecological disruption from climate change. *Nature*, *580*(7804), 496–501. https://doi.org/10.1038/s41586-020-2189-9

van Vuuren, D. P., Edmonds, J., Kainuma, M., Riahi, K., Thomson, A., Hibbard, K., et al. (2011). The representative concentration pathways: An overview. *Climatic Change*, *109*(1), 5–31. https://doi.org/10.1007/s10584-011-0148-z

von Schuckmann, K., Le Traon, P. Y., Smith, N., Pascual, A., Brasseur, P., Fennel, K., & Zuo, H. (2018). Copernicus marine service ocean state report. *Journal of Operational Oceanography*, *11*(sup1), S1–S142. https://doi.org/10.1080/1755876X.2016.1273446

Wagstaff, R. A. (1981). Low-frequency ambient noise in the deep sound channel—the missing component. *Journal of the Acoustical Society of America*, *69*(4), 1009–1014. https://doi.org/10.1121/1.385680

Wartzok, D., Popper, A. N., Gordon, J., & Merrill, J. (2003). Factors affecting the responses of marine mammals to acoustic disturbance. *Marine Technology Society Journal*, *37*(4), 6–15. https://doi.org/10.4031/002533203787537041

Zender, C. S., Vicente, P., & Wang, W. (2012). *Simplifying and accelerating model evaluation by NASA satellite data*. Paper Presented at The Earth Science Data Systems Working Group (ESDSWG) Meeting, November 13–15, 2012.